HCN Synthesis from Methane and Ammonia: Mechanisms of Pt+-Mediated C−N Coupling

Martin Diefenbach, Mark Brönstrup, Massimiliano Aschi,[†] Detlef Schröder, and Helmut Schwarz*

Contribution from the Institut für Organische Chemie, Technische Universität Berlin, Strasse des 17 Juni 135, D-10623 Berlin, Germany

Received July 26, 1999

Abstract: The Pt+-mediated coupling of methane and ammonia has been studied both experimentally and computationally. This system serves as a model for the Degussa process for the industrial production of the valuable feedstock hydrogen cyanide. Mass spectrometric studies demonstrate that C−N bond formation is catalyzed efficiently by Pt+. Details of the experimentally observed reaction channels have been explored computationally using the B3LYP hybrid DFT/HF functional. In the first reaction step, Pt+ dehydrogenates CH_4 to yield $PtCH_2^+$; in contrast, dehydrogenation of ammonia by Pt+ is endothermic and does not occur experimentally. Starting from $PtCH_2^+$ and NH_3, C−N bond formation, which constitutes the crucial step in making HCN from CH_4 and NH_3, is achieved via two independent pathways. The major pathway is found to be exothermic by 23 kcal mol^{-1} and yields neutral PtH and $CH_2NH_2^+$. The second pathway involves a dehydrogenation to yield the aminocarbene complex $PtC(H)NH_2^+$ ($\Delta_rH = -36$ kcal mol^{-1}); dehydrogenation of $PtC(H)NH_2^+$ to $PtCNH^+$ is exothermic with respect to $PtCH_2^+ + NH_3$ ($\Delta_rH = -8$ kcal mol^{-1}) but hindered by kinetic barriers. A comparison of Pt+ with other transition metal cations (Fe+, Co+, Rh+, W+, Os+, Ir+, and Au+) shows that Pt+ is unique with respect to its ability to activate 1 equiv of CH_4 *and* to mediate C−N bond coupling.

1. Introduction

The industrially important synthesis of hydrogen cyanide is commonly realized by coupling of methane with ammonia, i.e., $CH_4 + NH_3 \rightarrow HCN + 3H_2$. Although entropically favored, the net reaction is endothermic by 61 kcal mol^{-1}, and thus thermochemical equilibrium needs to be shifted toward the products by appropriate means. To this end, presently two concepts are pursued, both of which rely on platinum or rhodium as a catalyst. In the Degussa process (Scheme 1), a 1:1 mixture of methane and ammonia is passed through a Pt-coated tubewall reactor at rather high temperatures in order to overcome endothermicity, while in the Andrussow process, dioxygen is added to shift the energy balance by formation of water rather than molecular hydrogen. Despite the enormous relevance of both processes in industrial chemistry, mechanistic insight is still limited.[1−4]

In the present study, we investigate the Pt+-mediated coupling of methane and ammonia by a combination of mass-spectrometric experiments and ab initio theory applied to a model system with drastically reduced complexity. Although surface properties are not accounted for, the gas-phase reaction of bare platinum cations with methane and ammonia can serve as such a model, since insight into the *intrinsic* physical and chemical properties of the reactants, the nature of the intermediates, and,
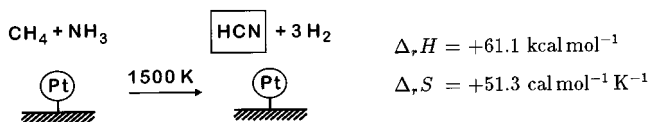
in particular, the role of the electronic structure of the metals is provided without complicating, interfering effects caused by the bulk. While the presence of a net Coulombic charge in the ion−molecule reactions might appear rather drastic, the active sites of solid-state catalysts may well contain cationic structures to some extent,[5] because point defects and linear, planar, or volumetric effects such as edge dislocations appear at finite temperatures.

In a recent communication,[6] we reported experiments on the Pt+/CH_4/NH_3 system (Scheme 2) using Fourier transform ion cyclotron resonance (FTICR) mass spectrometry, which are briefly summarized here. Bare platinum cations dehydrogenate methane in a fast reaction (rate constant $k_1 = 8.2 \times 10^{-10}$ cm^3 molecule^{-1} s^{-1}; efficiency[7] $\phi = 0.8$) to afford the cationic platinum carbene $PtCH_2^+$ (reaction 1). In contrast, interaction of Pt+ with ammonia (reaction 2) only results in slow ($k_2 \approx 5 \times 10^{-13}$ cm^3 molecule^{-1} s^{-1}; $\phi \leq 0.001$) formation of the $Pt(NH_3)^+$ adduct complex. However, $PtCH_2^+$ reacts rapidly ($k_3 = 6.2 \times 10^{-10}$ cm^3 molecule^{-1} s^{-1}; $\phi = 0.3$) with ammonia under formations of $CH_2NH_2^+$, $PtC(H)NH_2^+$, and NH_4^+ ac-

Scheme 1

$$\Delta_rH = +61.1 \text{ kcal mol}^{-1}$$
$$\Delta_rS = +51.3 \text{ cal mol}^{-1} \text{ K}^{-1}$$

* To whom correspondence should be addressed. Tel.: +49 30 314-23483. Fax: +49 30 314-21102. E-mail: schw0531@www.chem.tu-berlin.de.
† Present address: Dipartimento di Chimica, Universitá di Roma "La Sapienza", I-00185 Roma, Italy.
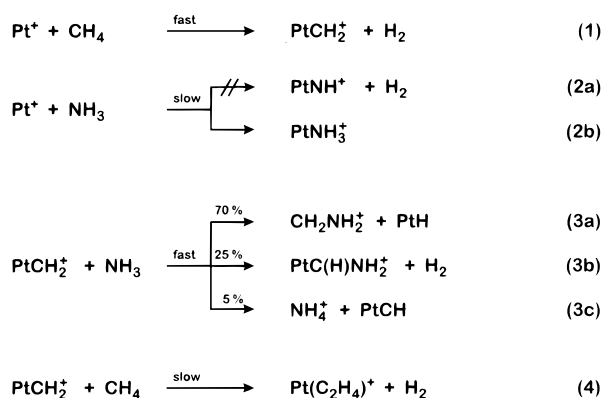
(1) Hasenberg, D.; Schmidt, L. D. *J. Catal.* **1985,** *91,* 116.
(2) Hasenberg, D.; Schmidt, L. D. *J. Catal.* **1986,** *97,* 156.
(3) Hasenberg, D.; Schmidt, L. D. *J. Catal.* **1987,** *104,* 441.
(4) Waletzko, N.; Schmidt, L. D. *AIChE J.* **1988,** *34,* 1146.

(5) Somorjai, G. A. *Introduction to Surface Chemistry and Catalysis*; Wiley: New York, 1994.
(6) Aschi, M.; Brönstrup, M.; Diefenbach, M.; Harvey, J. N.; Schröder, D.; Schwarz, H. *Angew. Chem., Int. Ed.* **1998,** *37,* 829.
(7) Given as $\phi = k_r/k_c$, where k_r is the experimentally observed rate constant and k_c is the collision rate constant derived from capture theory.[62−64]

Scheme 2

$$Pt^+ + CH_4 \xrightarrow{\text{fast}} PtCH_2^+ + H_2 \qquad (1)$$

$$Pt^+ + NH_3 \xrightarrow{\text{slow}} \begin{cases} \text{//} \rightarrow PtNH^+ + H_2 & (2a) \\ \rightarrow PtNH_3^+ & (2b) \end{cases}$$

$$PtCH_2^+ + NH_3 \xrightarrow{\text{fast}} \begin{cases} \xrightarrow{70\%} CH_2NH_2^+ + PtH & (3a) \\ \xrightarrow{25\%} PtC(H)NH_2^+ + H_2 & (3b) \\ \xrightarrow{5\%} NH_4^+ + PtCH & (3c) \end{cases}$$

$$PtCH_2^+ + CH_4 \xrightarrow{\text{slow}} Pt(C_2H_4)^+ + H_2 \qquad (4)$$

cording to reactions 3a–c in a ratio of 70:25:5. The secondary reaction (reaction 4) of $PtCH_2^+$ with another methane molecule to yield a Pt^+–ethene complex is too slow ($k_4 = 0.2 \times 10^{-10}$ cm^3 molecule^{-1} s^{-1}; $\phi = 0.02$) to compete with C–N bond formation in the presence of ammonia. The genesis and connectivities of the ions were elucidated by deuterium labeling experiments as well as B3LYP calculations. Concerning theory, up to this point information on the transition structures was not available; thus, a crucial feature in a more complete picture of the relevant reaction paths was missing.

Here, we describe a DFT/HF hybrid potential energy surface (PES) study of the relevant reaction paths at the B3LYP level, complemented by additional FTICR-MS experiments. The subject is well suited for a combined experimental and theoretical study, as both approaches treat the system under identical chemical conditions (strictly single-collision, bimolecular reactions) in the same environment, i.e., the gas phase.

2. Experimental Section

The experiments were performed with a Spectrospin CMS 47X FTICR mass spectrometer equipped with an external ion source and a superconducting magnet (Oxford Instruments; maximum field strength 7.05 T); the instrument and its operation have been described in detail before.[8,9] In brief, Pt^+ ions were generated by laser desorption/laser ionization from a pure platinum target and transferred through ion optics into the ICR cell. A computer-controlled ion-ejection protocol, FERETS,[10] was used to isolate the most abundant metal isotope, which was subsequently thermalized by collisions with argon as buffer gas. The mass-selected Pt^+ cation was then reacted with leaked-in ammonia or methane at pressures of $(5-10) \times 10^{-9}$ mbar. Similarly, $PtCH_2^+$ generated from thermalized Pt^+ with pulsed-in methane was subsequently reacted with leaked-in ammonia. $PtNH^+$ was produced by reacting Pt^+ with pulsed-in HN_3 gas in analogy to the recently described formation of $FeNH^+$.[11] For exploratory studies of other MCH_2^+/NH_3 systems, other precursors were used in part (see below); however, the major features of the experiments were identical to those performed on the Pt^+ system.

Rate constants and branching ratios were derived from the pseudo-first-order reaction kinetics following well-established routines. In the present system, formations of NH_4^+ and $CH_2NH_2^+$ as very low-mass ions compared to Pt^+ cause some increase of the experimental error because mass discrimination in detection is inevitable in FTICR mass spectrometry when ion masses differ largely. Various methods were applied to compensate for mass discrimination (e.g., variation of

excitation pulses, single-ion monitoring), and from the averaged data we assign errors of ±50% for the absolute rate constants and ±20% for the branching ratios. Note, however, that this source of error is, by and large, systematic and therefore affects the comparison of the MCH_2^+/NH_3 systems much less.

3. Computational Details

The PES was calculated with the B3LYP[12,13] DFT/HF hybrid functional as implemented in Gaussian 94.[14] Optimizations of minima as well as transition structures were carried out with double-ζ type basis sets including polarization functions (DZP). For hydrogen, carbon, and nitrogen, 6-31+G* basis sets were employed; for platinum we used the LANL2DZ pseudopotential for the inner 60 core electrons ([Kr]-$4d^{10}4f^{14}$) in order to account for scalar relativistic effects, combined with the associated LANL2DZ basis set. At the same level of theory, frequency calculations were performed in order to identify the stationary points as local minima, transition structures, or higher order saddle points.

Energetics and population analyses were computed as single points on the optimized geometries, with the larger 6-311+G** triple-ζ basis sets on the nonmetals and an extended basis set[15] on Pt, including f-polarization functions in conjunction with the LANL2DZ pseudopotential. These basis sets will be referred to as TZP. The energies were corrected for zero-point vibrational energy (ZPVE) using the unscaled results from the frequency calculations at the DZP level.

The level of theory applied cannot be expected to yield as accurate thermochemical data as reported for the 3d transition metal series,[16,17] because relativistic effects[18-21] are substantial for platinum, and the pseudopotential used only covers scalar relativistic effects to a first approximation, neglecting spin–orbit effects. Therefore, the energetic data should not be regarded as quantitatively rigorous; rather, they form the basis for a reasonable mechanistic description of the potential energy surfaces involved with respect to the structural features of the minima and particularly the energy demands of the associated transition structures.

4. Results

In the following sections, we first present experimental results of the $Pt^+/CH_4/NH_3$ couple and some closely related systems. The next section deals with the theoretical investigation of the potential energy surfaces of the relevant reaction paths for C–N bond coupling in the reaction of $PtCH_2^+$ with NH_3. Finally, experimental and theoretical results are discussed in comparison, and some mechanistic predictions are made in order to allow the assessment of the relevance of our simplified gas-phase model for the Degussa process.

(8) Eller, K.; Schwarz, H. *Int. J. Mass Spectrom. Ion Processes* **1989**, *93*, 243.

(9) Eller, K.; Zummack, W.; Schwarz, H. *J. Am. Chem. Soc.* **1990**, *112*, 621.

(10) Forbes, R. A.; Laukien, F. H.; Wronka, J. *Int. J. Mass Spectrom. Ion Processes* **1988**, *83*, 23.

(11) Brönstrup, M.; Kretzschmar, I.; Schröder, D.; Schwarz, H. *Helv. Chim. Acta* **1998**, *81*, 2348.

(12) Becke, A. D. *J. Chem. Phys.* **1993**, *98*, 5648.

(13) Stephens, P. J.; Devlin, F. J.; Frisch, M. J.; Chabalowski, C. F. *J. Phys. Chem.* **1994**, *98*, 11632.

(14) Frisch, M. J.; Trucks, G. W.; Schlegel, H. B.; Gill, P. M. W.; Johnson, B. G.; Robb, M. A.; Cheeseman, J. R.; Keith, T.; Petersson, G. A.; Montgomery, J. A.; Raghavachari, K.; Al-Laham, M. A.; Zakrzewski, V. G.; Ortiz, J. V.; Foresman, J. B.; Cioslowski, J.; Stefanov, B. B.; Nanayakkara, A.; Challacombe, M.; Peng, C. Y.; Ayala, P. Y.; Chen, W.; Wong, M. W.; Andres, J. L.; Replogle, E. S.; Gomperts, R.; Martin, R. L.; Fox, D. J.; Binkley, J. S.; Defrees, D. J.; Baker, J.; Stewart, J. P.; Head-Gordon, M.; Gonzalez, C.; Pople, J. A. *Gaussian 94*, Revision E.1; Gaussian, Inc.; Pittsburgh, PA, 1995.

(15) Pavlov, M.; Blomberg, M. R. A.; Siegbahn, P. E. M.; Wesendrup, R.; Heinemann, C.; Schwarz, H. *J. Phys. Chem. A* **1997**, *101*, 1567.

(16) Glukhovtsev, M. N.; Bach, R. D.; Nagel, C. J. *J. Phys. Chem. A* **1997**, *101*, 316.

(17) Kellogg, C. B.; Irikura, K. K. *J. Phys. Chem. A* **1999**, *103*, 1150.

(18) Pyykkö, P. *Chem. Rev.* **1988**, *88*, 563. In addition, a list of 9438 (as of July 1999) references concerning the relativistic treatment of atoms and molecules may be found on the Internet at http://www.csc.fi/lul/rtam/.

(19) Kaltsoyannis, N. *J. Chem. Soc., Dalton Trans.* **1996**, *1*, 1.

(20) Hess, B. A.; Marian, C. M.; Peyerimhoff, S. D. Ab initio calculation of spin–orbit effects in molecules including electron correlation. In *Modern Electronic Structure Theory*; Yarkony, D. R., Ed.; World Scientific: Singapore, 1995; Part I, p 152.

(21) Hess, B. A. *Ber. Bunsen-Ges. Phys. Chem.* **1997**, *101*, 1.

4.1. Experiments. Various aspects of reactions 1, 3, and 4 have already been reported.[6,15,22-26] As the C−N bond coupling in reaction 3 constitutes the central part of the theoretical discussion, the key issues are briefly summarized. Further, some details of the consecutive reactions in the $Pt^+/CH_4/NH_3$ system are included here, which were not fully described in our previous communication,[6] and these results are complemented by a reactivity study of the $PtNH^+$ cation. An additional section is devoted to assess whether the metal-mediated C−N bond formation is specific for platinum compared to some other transition metals.

In reaction 3a, $PtCH_2^+$ and NH_3 react under C−N bond formation to give neutral PtH and protonated formimine $CH_2NH_2^+$. The isomeric species CH_3NH^+ and $CHNH_3^+$ are assumed to be far less stable and thus excluded from further consideration. The connectivity of the ionic product $CH_2NH_2^+$ is supported by deuterium labeling in that $PtCD_2^+$ and NH_3 give solely loss of PtH and formation of $CD_2NH_2^+$ for channel 3a; the latter ion undergoes specific proton transfer with NH_3 to form NH_4^+ concomitant with neutral CD_2NH.

The aminocarbene structure $PtC(H)NH_2^+$ for the ionic product of reaction 3b has been deduced in a similar fashion. Upon reacting $PtCD_2^+$ with NH_3, only HD loss is observed in channel 3b. This finding rules out a formimine complex $Pt(CD_2NH)^+$, because formation of this isomer would imply H_2 rather than HD loss from the $PtCD_2^+/NH_3$ reactants. Subsequent ion/molecule reactions of $PtC(D)NH_2^+$ with ammonia exclusively yield the diaminocarbene complex $PtC(NH_2)_2^+$ and HD. This result demonstrates a nonequivalence of hydrogen and deuterium atoms in the ionic reactant and thus supports the $PtC(D)NH_2^+$ structure. Another indication for the platinum aminocarbene structure is provided by collision-induced dissociation (CID) experiments.[27,28] CID of $PtC(D)NH_2^+$ with argon yields $[Pt,C,N,H]^+$, Pt^+, and a $[C,N,H_2,D]^+$ fragment. These results disfavor Pt-centered structures with N−Pt−C connectivity or platinum−hydrogen-bonded structures as products of reaction 3b. Furthermore, specific loss of HD from $PtC(D)NH_2^+$ implies formation of an isonitrile complex $PtCNH^+$ rather than its isomer $PtNCH^+$. CID of the platinum diaminocarbene cation $PtC(NH_2)_2^+$ leads to the neutral fragments $[C,N_2,H_4]$, NH_3, and $[H,C,N]$, corresponding to detection of Pt^+, $[Pt,C,N,H]^+$, and $[Pt,N,H_3]^+$, respectively (relative intensities 100/40/15). The fact that loss of the complete ligand is most abundant indicates a monoligated platinum complex, whereas for a bisligated species, e.g., $Pt(CNH)(NH_3)^+$, one should expect prevalence of the singly ligated fragments $PtCNH^+$ and $PtNH_3^+$. Nevertheless, observation of losses of NH_3 and HCN indicates some sort of a collision-induced isomerization between $PtC(NH_2)_2^+$ and $Pt(CNH)(NH_3)^+$ on its way to dissociation. The diaminocarbene complex $PtC(NH_2)_2^+$ undergoes solely adduct formation with another equivalent of ammonia, whereas further reactions, e.g., ligand exchange to yield $Pt(NH_3)_n^+$ ($n = 1, 2$), are not observed.

To probe the collision-induced formation of $PtCNH^+$ in more detail, we studied the reaction of bare Pt^+ with methylamine. The entrance energy of the Pt^+/CH_3NH_2 system ($\sum\Delta_f H = 328$ kcal mol^{-1})[29] is somewhat higher than that of the $PtCH_2^+/NH_3$ couple ($\sum\Delta_f H = 303$ kcal mol^{-1}).[29-31] The difference of 25 kcal mol^{-1} is apparently sufficient to overcome the barriers associated with the second H_2 loss (see below). Thus, $PtCNH^+$ (10%) is observed as a product ion, in addition to the formations of $CH_2NH_2^+$ (80%) and $PtC(H)NH_2^+$ (10%), which are in perfect analogy with reaction 3. If CD_3NH_2 is used, again in analogy to reaction 3, only PtD, D_2, and D_2 + HD are lost as neutral fragments, concomitant with formations of $CD_2NH_2^+$, $PtC(D)NH_2^+$, and $PtCNH^+$, respectively. The fact that, after double dehydrogenation, no deuterium label is retained in the Pt^+ product supports the generation of the isonitrile complex $PtCNH^+$ rather than $PtNCH^+$. Furthermore, C−N bond formation to yield $PtC(H)NH_2^+$ is also observed in the reaction of $PtCH_2^+$ and methylamine, but with much lower yields.[32]

$[Pt,C,N,H]^+$ ions, generated by CID from $PtC(H)NH_2^+$, were reisolated and submitted to a second collisional activation experiment, which yields exclusively Pt^+ and neutral $[H,C,N]$. Experiments aimed to distinguish directly between $PtCNH^+$ and $PtNCH^+$ ions generated from different precursors (i.e., CID of $PtC(H)NH_2^+$ stemming from $Pt^+/CH_4/NH_3$, and the $[Pt,C,N,H]^+$ ions derived from Pt^+/CH_3NH_2 and Pt^+/t-C_4H_9CN), were inconclusive. Thus, ligand detachment prevails, while structurally indicative fragments such as PtC^+ or PtN^+ were negligible upon CID. Despite this failure, regeneration of Pt^+ upon CID of $[Pt,C,N,H]^+$ demonstrates that liberation of the ligand−either as HCN or as HNC−from the metal is feasible (see below).

Reaction of Platinum Cation and Ammonia. A key feature in the gas-phase model of the Degussa process is the high selectivity of Pt^+ for activating methane, followed by the preferential coupling of the $PtCH_2^+$ complex with NH_3 rather than CH_4. Obviously, the alternative reverse sequence, that is, (i) initial Pt^+-mediated activation of NH_3 and (ii) coupling of the ionic product with CH_4, has to be considered also. However, formation of $PtNH^+$ (reaction a) is not observed, and it is interesting to know whether this nonoccurrence is due to thermodynamic or kinetic restrictions. To probe this issue, we investigated the reversal of ammonia activation, i.e., reaction 5.

$$PtNH^+ + H_2 \longrightarrow Pt^+ + NH_3 \qquad (5)$$

The fact that reaction 5 occurs under FT-ICR conditions with a rate constant of $k = 4.4 \times 10^{-10}$ cm^3 molecule^{-1} s^{-1} ($\phi = 0.3$) demonstrates that the nonoccurrence of reaction 2a is definitely endothermic. Thus, irrespective of any additional activation barriers, dehydrogenation of ammonia by Pt^+ is prevented by a thermochemical restriction. Note that this result is in accord with the decrease of the bond strengths from $D_0(Pt^+-CH_2) = 113$ kcal mol^{-1} [15] to $D_0(Pt^+-NH) = 84$ kcal mol^{-1} [6] and $D_0(Pt^+-O) = 77$ kcal mol^{-1}.[15] In the reaction of $PtNH^+$ with D_2, no distinct intermolecular isotope effects are observed ($k_H/k_D = 1.0 \pm 0.2$), indicating that thermochemistry predominates, as in the related $Pt^+ + CH_4 \rightleftharpoons PtCH_2^+ + H_2$ system.[25]

Although $PtNH^+$ does not play any role in our $Pt^+/CH_4/NH_3$ model system within the energy frame of the present FTICR

(22) Irikura, K. K.; Beauchamp, J. L. *J. Am. Chem. Soc.* **1989**, *111*, 75.

(23) Irikura, K. K.; Beauchamp, J. L. *J. Am. Chem. Soc.* **1991**, *113*, 2769.

(24) Irikura, K. K.; Beauchamp, J. L. *J. Phys. Chem.* **1991**, *95*, 8344.

(25) Wesendrup, R.; Schröder, D.; Schwarz, H. *Angew. Chem., Int. Ed. Engl.* **1994**, *33*, 1174.

(26) Heinemann, C.; Hertwig, R. H.; Wesendrup, R.; Koch, W.; Schwarz, H. *J. Am. Chem. Soc.* **1995**, *117*, 495.

(27) Burnier, R. C.; Cody, R. B.; Freiser, B. S. *J. Am. Chem. Soc.* **1982**, *104*, 7436.

(28) Cody, R. B.; Freiser, B. S. *Int. J. Mass Spectrom. Ion Phys.* **1982**, *41*, 199.
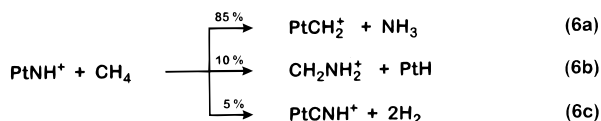
(29) Lias, S. G.; Bartmess, J. E.; Liebman, J. F.; Holmes, J. L.; Levin, R. D.; Mallard, W. G. *J. Phys. Chem. Ref. Data* **1988**, *17*, Suppl. 1. Part of the compilation is available on the Internet at http://webbook.nist.gov/chemistry/.

(30) Heinemann, C.; Wesendrup, R.; Schwarz, H. *Chem. Phys. Lett.* **1995**, *239*, 75.

(31) Heinemann, C.; Schwarz, H.; Koch, W.; Dyall, K. G. *J. Chem. Phys.* **1996**, *104*, 4642.

(32) Brönstrup, M.; Schröder, D.; Schwarz, H. *Organometallics* **1999**, *18*, 1939.

experiments, one might conceive formation of platinum imines at higher energies, as they do exist in the rather drastic conditions of the Degussa process. To probe if carbon–nitrogen bond coupling can also be achieved starting from PtNH$^+$, we investigated the reaction of PtNH$^+$ with CH$_4$. In close analogy to the related PtO$^+$ cation,[15] PtNH$^+$ reacts efficiently with methane ($k = 5.9 \times 10^{-10}$ cm^3 molecule^{-1} s^{-1}; $\phi = 0.6$) according to reaction 6.[33]

$$
\text{PtNH}^+ + \text{CH}_4 \quad
\begin{array}{ll}
\xrightarrow{85\%} & \text{PtCH}_2^+ + \text{NH}_3 \quad (6a) \\
\xrightarrow{10\%} & \text{CH}_2\text{NH}_2^+ + \text{PtH} \quad (6b) \\
\xrightarrow{5\%} & \text{PtCNH}^+ + 2\text{H}_2 \quad (6c)
\end{array}
$$

Although some C–N coupling is observed in reactions 6b and 6c, it turns out that the main products are PtCH$_2^+$ and ammonia, which are the reagents of reaction 3 and thus do not open a new pathway for HCN formation. In other words, even if ammonia were activated by platinum under more drastic conditions, the metal imine species undergoes rapid metathesis to the corresponding carbene in the presence of methane. Alternatively, the metal imine might react with an excess of ammonia. In the gas phase, PtNH$^+$ is rapidly deprotonated by NH$_3$ to yield NH$_4^+$ and PtN; this process resembles the thermal decomposition of ammonia to nitrogen under heterogeneous conditions.

Variation of the Metal. A pivotal question is whether the gas-phase process of carbon–nitrogen coupling is confined to platinum, or if other metal cations also mediate C–N bond formation by the same mechanism. Therefore, the extension of the concept

$$
\text{"M}^+ \xrightarrow{\text{CH}_4} \text{MCH}_2^+ \xrightarrow{\text{NH}_3} \text{C–N coupling products"}
$$
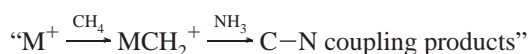
to other transition metals has been explored briefly. On thermochemical grounds, dehydrogenation of methane to yield the corresponding metal carbenes is feasible for the late 5d elements Ta, W, Os, Ir, and Pt only,[22–25] while all other singly charged d-block metals proved to be unreactive;[34] the actinide cation Th$^+$ also activates methane though with low efficiency.[35] Accordingly, the metal–carbene cations have to be generated by other means in order to investigate their reactivity toward ammonia. The scope of metal variation is therefore limited to those metals for which carbene generation could be achieved in reasonable yields, i.e., Fe$^+$, Co$^+$, Rh$^+$, W$^+$, Os$^+$, Ir$^+$, Pt$^+$, and Au$^+$. The product distributions of the reactions of MCH$_2^+$ and NH$_3$ are given in Table 1.

The carbenes of the 3d metals Fe$^+$ and Co$^+$ are completely unreactive toward ammonia. This cannot be rationalized by the related metal–carbene bond strengths, as the carbenes of the 5d homologues of Fe and Co, i.e., Os and Ir, react efficiently with ammonia (see below), although the release of the carbene unit is easier for 3d metals than for 5d metals,[36] i.e., $D_0(\text{Fe}^+\text{–CH}_2) = 82$ kcal mol^{-1} vs $D_0(\text{Os}^+\text{–CH}_2) = 113$ kcal mol^{-1}, and $D_0(\text{Co}^+\text{–CH}_2) = 76$ kcal mol^{-1} vs $D_0(\text{Ir}^+\text{–CH}_2) = 123$ kcal mol^{-1}. Moreover, the fact that FeCH$_2^+$ and CoCH$_2^+$ are able to activate several small alkanes and alkenes[37] dem-

---

(33) Formation of up to 10% Pt$^+$ + CH$_3$NH$_2$ cannot be excluded. However, reactions of PtNH$^+$ with background contaminants from pulsed-in HN$_3$ used to generate PtNH$^+$ [11] also yield Pt$^+$, and a quantification of this channel is prevented.

(34) Schwarz, H. *Angew. Chem., Int. Ed. Engl.* **1991**, *30*, 820.

(35) Marçalo, J.; Leal, J. P.; Pires de Matos, A. *Int. J. Mass Spectrom. Ion Processes* **1996**, *157/158*, 265.

(36) Freiser, B. S., Ed. *Organometallic Ion Chemistry*; Kluwer: Dordrecht, 1996.

Table 1. Reaction Efficiencies (ϕ_{NH_3})^a and Product Branching Ratios^b for the Reactions of Cationic Transition Metal Carbenes^c with Ammonia, and Relative Efficiencies for Methane/Ammonia Coupling^d with $\phi_{\text{rel}}(\text{Pt}) = 100$

		ionic reaction products^b				
MCH$_2^+$	$\phi_{\text{NH}_3}{}^a$	NH$_4^+$	CH$_2$NH$_2^+$	M$^+$	MC(H)NH$_2^+$	$\phi_{\text{rel}}{}^d$
FeCH$_2^+$	0.0^e					0
CoCH$_2^+$	0.0^e					0
RhCH$_2^+$	0.1			75	25^f	0
WCH$_2^+$	0.1				100^f	6
OsCH$_2^+$	0.2	45			55^f	19
IrCH$_2^+$	0.4	60			40^f	65
PtCH$_2^+$	0.3	5	70		25	100
AuCH$_2^+$	0.6		100			0

^{a} Given as $\phi = k_r/k_c$, where k_r is the experimentally observed rate constant and k_c is the collision rate constant derived from capture theory.[62–64] ^{b} Branching ratios normalized to a sum of 100%. ^{c} The following precursor systems were used to generate the metal carbene cations: Fe$^+$/C$_2$H$_4$/N$_2$O; Co$^+$/C$_7$H$_8$; Rh$^+$/c-C$_3$H$_6$; W$^+$/CH$_4$; Os$^+$/CH$_4$; Ir$^+$/CH$_4$; Pt$^+$/CH$_4$; Au$^+$/CH$_3$Cl. ^{d} Derived from reaction efficiencies for methane activation by bare M$^+$ cations (ϕ_{CH_4}) and ammonia activation by MCH$_2^+$ (ϕ_{NH_3}), and branching ratios (BR) for C–N coupling, $\phi_{\text{rel}} = N\phi_{\text{CH}_4}\phi_{\text{NH}_3}(1 - \text{BR}_{\text{NH}_4^+}/100)$, with normalization constant $N = 585$. For M = W, Os, and Ir, ϕ_{CH_4} is taken from ref 23; for M = Pt, ϕ_{CH_4} is the average of the values given in refs 23 and 25. ^{e} Below the detection limit, i.e., $k_r/k_c < 0.01$. ^{f} Ion structure not established (see text).

onstrates that these carbenes are not unreactive in general. Obviously, nucleophilic attack of the 3d metal carbenes by ammonia is hampered compared to that of the higher homologues. Lack of reactivity also cannot be ascribed to a mere charge effect, because comparable theoretical calculations performed for FeCH$_2^+$, CoCH$_2^+$, NiCH$_2^+$, and their 5d counterparts indicate that the late 3d metal carbenes possess higher partial charges on carbon than their 5d congeners.[26,38] Thus, the reaction of MCH$_2^+$ with NH$_3$ as a rather soft nucleophile appears to be orbital-controlled. The larger polarizabilities of the 5d metals as well as their more effective π-bonding facilitate nucleophilic attack at the π-system and may thus account for the observed differences in reactivity.

The carbenes of the 4d and 5d metals Rh, W, Os, and Ir show moderate efficiencies in their reactions with ammonia. The major pathway in the reaction of RhCH$_2^+$ and NH$_3$ yields Rh$^+$, a product channel that is not observed for platinum and the other 5d metals. Although the neutral products cannot be detected directly, conceivable species such as CH$_2$NH + H$_2$ or the ylid $^-$CH$_2^+$NH$_3$ are disfavored on energetic grounds. According to thermochemical data, exothermic formation of methylamine from MCH$_2^+$ + NH$_3$ requires metals with $D_0(\text{M}^+\text{–CH}_2) < 87$ kcal mol^{-1}, which explains that it is only observed for RhCH$_2^+$ ($D_0 = 85$ kcal mol^{-1}) and for none of the 5d metal carbenes. There exist two obvious mechanistic scenarios for metal-mediated CH$_3$NH$_2$ formation in the MCH$_2^+$/NH$_3$ systems (Scheme 3). With regard to the rhodium case,[39] these are (i) a direct nucleophilic attack of ammonia at carbon to yield a C–N-bonded RhCH$_2$NH$_3^+$ intermediate, followed by successive H-transfers to yield Rh(CH$_3$NH$_2$)$^+$ as the product complex, and (ii) formation of a metal-centered ion–dipole complex between NH$_3$ and the metal carbene, followed by a metal-assisted hydrogen transfer to yield a bisligated methyl amido complex, which may liberate methylamine by reductive elimination. Both routes involve Rh(CH$_3$NH$_2$)$^+$ as common intermediate, and presently no preference for either route can be made. The minor [Rh,C,N,H$_3$]$^+$ product dissociates into [Rh,C,N,H]$^+$ and Rh$^+$

---

(37) Buckner, S. W.; Freiser, B. S. *Polyhedron* **1988**, *7*, 1583.

(38) Holthausen, M. C.; Mohr, M.; Koch, W. *Chem. Phys. Lett.* **1995**, *240*, 245.

(39) Tolbert, M. A.; Beauchamp, J. L. *J. Phys. Chem.* **1986**, *90*, 5015.

Scheme 3
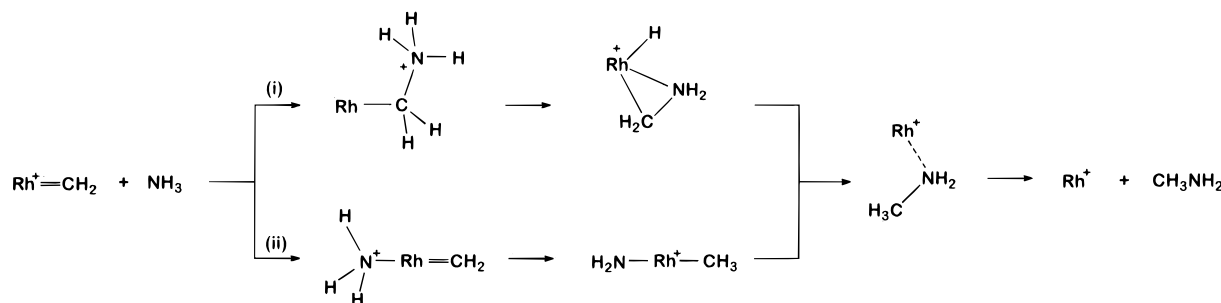
upon CID, and we tentatively assign a rhodium−aminocarbene structure analogous to PtC(H)NH$_2^+$ (see above). The formation of CH$_2$NH$_2^+$ and neutral MH, i.e., the main product channel of the PtCH$_2^+$/NH$_3$ couple, is not observed for rhodium, which is completely in line with thermochemical considerations that predict, for this particular metal, an endothermicity of 10 kcal mol^{-1} for this channel.

Only two reaction pathways are observed for the 5d metal carbenes WCH$_2^+$, OsCH$_2^+$, and IrCH$_2^+$, i.e., an acid−base reaction to yield NH$_4^+$ concomitant with neutral MCH and dehydrogenation, presumably leading to the corresponding aminocarbenes MC(H)NH$_2^+$. Consecutively, these ions react with excess NH$_3$ to yield [M,C,N$_2$,H$_4$]$^+$ concomitant with loss of H$_2$. This behavior is analogous to the PtCH$_2^+$/NH$_3$ couple, and we therefore tentatively propose bisaminocarbene structures MC(NH$_2$)$_2^+$ for these ionic reaction products. Note, however, that some H/D scrambling occurs with MCD$_2^+$/NH$_3$ for M = Os and Ir, while this is absent for M = Pt. For osmium and iridium, large fractions of the carbenes are consumed by the simple acid−base reaction with ammonia to afford MCH species. Conceptually, these carbyne species can be considered as precursors for soot formation such that the catalytic activity of these metals appears limited, judged on these particular gas-phase experiments. Although proton transfer from MCH$_2^+$ to ammonia is absent for tungsten, its high oxophilicity prompts efficient side reactions with background contaminants, like water or oxygen, to yield [W,C,O,H$_2$]$^+$ and WO$_2^+$, which renders further investigations difficult. Likewise, the catalytic activity of tungsten is likely to be limited by irreversible oxide formation with impurities, even under the drastic conditions of the Degussa process.

The reaction of AuCH$_2^+$ and NH$_3$ yields exclusively CH$_2$NH$_2^+$ and neutral AuH with high efficiency; neither the acid−base reaction nor aminocarbene formation is observed. Thus, the most remarkable trend upon moving to heavier elements across the 5d series concerns the decreasing branching ratio of aminocarbene vs metal hydride formation. This trend nicely agrees with the reaction enthalpies for formation of CH$_2$NH$_2^+$ and neutral MH, which are negative for the late 5d metals Ir, Pt, and Au only (Table 2). Note that the reaction enthalpies depend on the amount of energy needed for the release of the methylene unit from MCH$_2^+$, the amount of energy gained from metal hydride bond formation, and the ionization energy of the metal M. Thus, the above reaction is the most exothermic for gold, since D_0(Au$^+$−CH$_2$) is comparatively small while the Au−H bond strength and the first ionization energy of the gold atom are quite large.

In comparison, the moderate exothermicity for the IrCH$_2^+$/NH$_3$ couple does not suffice for formation of CH$_2$NH$_2^+$ and IrH, whereas Au$^+$ is not capable of activating methane. Therefore, it is tempting to speculate that the unique reactivity of the platinum cation, i.e., a combination of methane activation

Table 2. Ionization Energies IE(M),[a] Dissociation Energies D_0(M$^+$−CH$_2$) and D_0(M−H), and Enthalpies[b] for the Reaction MCH$_2^+$ + NH$_3$ → CH$_2$NH$_2^+$ + MH in kcal mol^{-1}

metal	IE(M)	D_0(M$^+$−CH$_2$)[c]	D_0(M−H)	$\Delta_r H$
Fe	182.2	81.5	34.5[c]	17.9
Co	181.7	75.9	43.0[c]	4.3
Rh	172.0	85.1	55.8[c]	10.4
W	184.0	111.0	62.9[e]	17.2
Os	200.6	113.0	60.5[e]	5.0
Ir	209.8	123.0	74.4[e]	−8.1
Pt	207.5	112.5[d]	78.1[f,g]	−20.0[i]
Au	212.7	94.0	77.5[h]	−43.1

[a] Reference 29. [b] Calculated from thermochemical cycles using heats of formation of M, M$^+$, CH$_2$ NH$_2^+$, NH$_3$, CH$_2$, and H (ref 29) and bond energies of MCH$_2^+$ and MH. [c] Reference 36. [d] Reference 15. [e] Reference 41 (DK-MCPF calculations). [f] This work. [g] D_0(Pt−H) = 74 kcal mol^{-1} was predicted in ref 41. [h] Reference 65. [i] −16 kcal mol^{-1} according to ref 41.

with selective and efficient carbon−nitrogen coupling of the PtCH$_2^+$ carbene with NH$_3$ in the gas-phase model, is also responsible for the outstanding role of platinum as catalyst in the Degussa process.

4.2. Calculations. C−H bond activation of methane by bare Pt$^+$ to afford PtCH$_2^+$ has formed the subject of numerous previous experimental and theoretical studies.[15,22−26,30,31] Therefore, our theoretical investigation is focused on the C−N coupling with PtCH$_2^+$ and NH$_3$ in reactions 3a and 3b. Reaction 3c, to afford NH$_4^+$ and neutral PtCH, is predicted to be almost thermoneutral ($\Delta_r H$ = 2 kcal mol^{-1}) at the B3LYP level of theory; as this simple proton transfer does not involve C−N bond formation, it is not considered any further. The calculations on reactions 3a and 3b are oriented toward the experimental results, and reaction paths which can be definitely excluded have not been pursued theoretically. The aim of the calculations is therefore to complement the experimental studies by supplying the missing information about the mechanistic details, i.e., geometric and electronic structures, thermochemistry, and in particular barriers en route to the products.

Potential−Energy Surfaces. A first and important finding of the computations is that all reactions considered in the PtCH$_2^+$/NH$_3$ couple can be explained by solely involving the doublet spin surface. Quartet states of all minima are found to be higher in energy than the relevant doublet transition structures mentioned below. Accordingly, spin multiplicities other than doublet do not seem to play a role under thermal conditions and are not pursued any further. Note, however, that the LS coupling scheme, which treats spin as a "good" quantum number, is not necessarily applicable for open-shell platinum compounds, and the energetics may vary moderately upon appropriate inclusion of spin−orbit coupling.

PES of Reactions 3a and 3b. Let us first address the major route, i.e., formation of an iminium cation and neutral PtH (Figures 1 and 2), according to reaction 3a. Under gas-phase
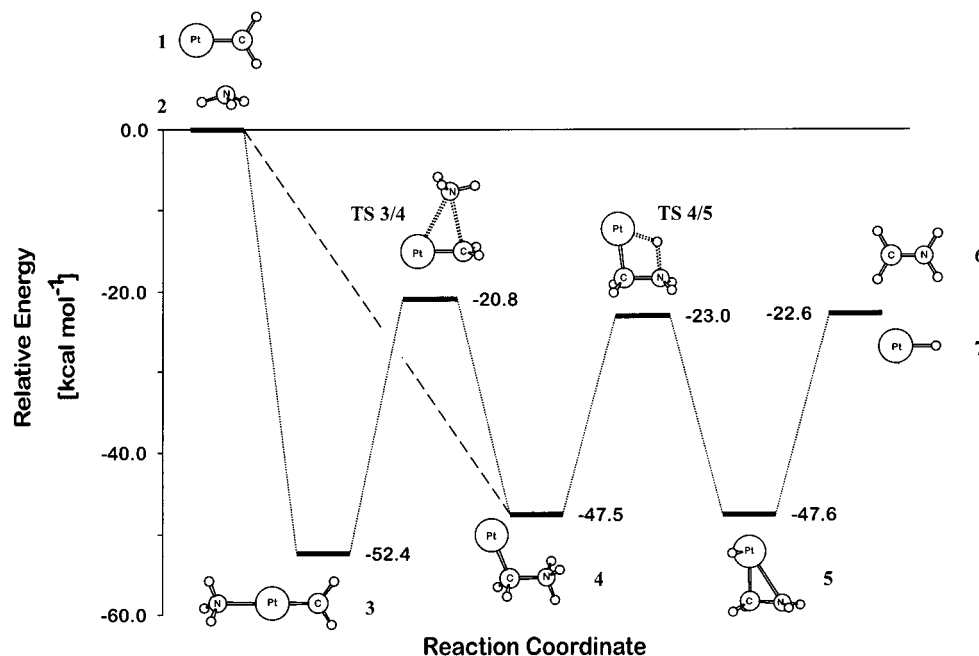
Figure 1. PES of reaction 3a calculated at the B3LYP/TZP//B3LYP/DZP level including ZPVE; charges are omitted.
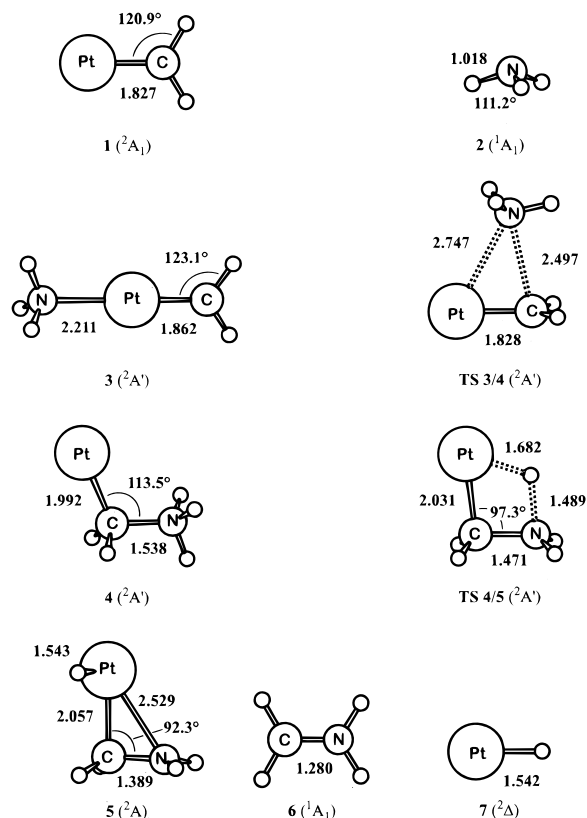

Figure 2. Calculated structures involved in reaction 3a. Bond lengths are given in angstroms and angles in degrees; electronic states are in parentheses.

Table 3. Mulliken Atomic Spin Densities on Pt, C, and N (ρ_i) and NBO Partial Charges (q_i), with Partial Charges of Hydrogens Summed into Adjacent Heavy Atom Pt, C, and N, Respectively

species	Mulliken spin densities			NBO partial charges		
	ρ_{Pt}	ρ_C	ρ_N	q_{Pt}	q_C	q_N
PtNH₃⁺	0.93		0.07	0.70		0.30
1	0.85	0.14		0.71	0.29	
3	0.94	0.07	−0.02	0.70	0.14	0.16
TS 3/4	0.77	0.12	0.11	0.54	0.21	0.25
4	0.90	0.07	0.04	0.39	0.01	0.61
TS 4/5	0.71	0.10	0.17	0.70	0.20	0.10
5	0.67	−0.03	0.32	0.57	0.26	0.17
TS 4/10	0.84	0.11	0.07	0.45	0.55	0.00
TS 4/8	0.39	0.67	−0.03	0.43	−0.03	0.61
8	0.18	0.84	−0.04	0.37	0.04	0.59
TS 8/9	0.20	0.76	−0.02	0.77	0.21	0.01
9	0.87	0.13	0.00	0.60	0.20	0.21
5/9	0.85	0.07	0.09	0.59	0.23	0.19
10	0.83	0.15	0.01	0.53	0.26	0.21
TS 10/12	0.43	0.54	−0.07	0.65	0.18	0.17
12	0.31	0.66	−0.08	0.54	0.31	0.15
TS 12/14	0.37	0.48	0.08	0.89	0.35	−0.24
TS 10/13	0.63	0.08	0.20	0.80	0.35	−0.15
13	0.67	−0.07	0.30	0.71	0.33	−0.05
TS 13/14	0.90	0.02	0.08	0.70	0.27	0.02
14	0.82	0.15	0.03	0.72	0.28	0.00
15	0.79	0.18	0.03	0.71	0.30	−0.01
PtNCH⁺	0.87	−0.03	0.15	0.85	0.63	−0.49
16	1.01	−0.01	−0.01	0.70	0.54	−0.24
17	0.61	−0.05	0.40	0.75	0.35	−0.10
20	0.87	0.05	0.03	0.47	0.34	0.09

conditions, the cationic platinum carbene **1** may be attacked by ammonia **2** either at the metal center to give **3** or at the carbon atom to give **4**. The former possibility seems more probable for an ion−dipole interaction since the positive charge of **1** is mainly located on Pt according to NBO partial charges (q_{Pt} = 0.71, see Table 3). Formation of **3** from the separated reactants releases 52 kcal mol⁻¹ complexation energy. The Pt−N bond length in **3** (r_{Pt-N} = 2.21 Å) is 0.17 Å larger than that in PtNH₃⁺ (r_{Pt-N} = 2.04 Å), and NBO analysis reveals a Pt−C double

bond and only a donor−acceptor interaction between platinum and nitrogen. These structural features are in keeping with the description of **3** as an ion−dipole complex between PtCH₂⁺ and NH₃. This notion is further supported by the significant difference of the corresponding Pt−N bond dissociation energies, i.e., D_0(H₃N−PtCH₂⁺) = 52 kcal mol⁻¹ vs D_0(H₃N−Pt⁺) = 74 kcal mol⁻¹. The barrier for NH₃ migration from platinum to carbon via **TS 3/4** amounts to 32 kcal mol⁻¹, thus being well below the energy of the entrance channel for isolated PtCH₂⁺ + NH₃. In **4**, which is only 5 kcal mol⁻¹ less stable than **3**, and which we assume to be also directly accessible by nucleophilic attack of the carbene fragment without a barrier (dashed line in
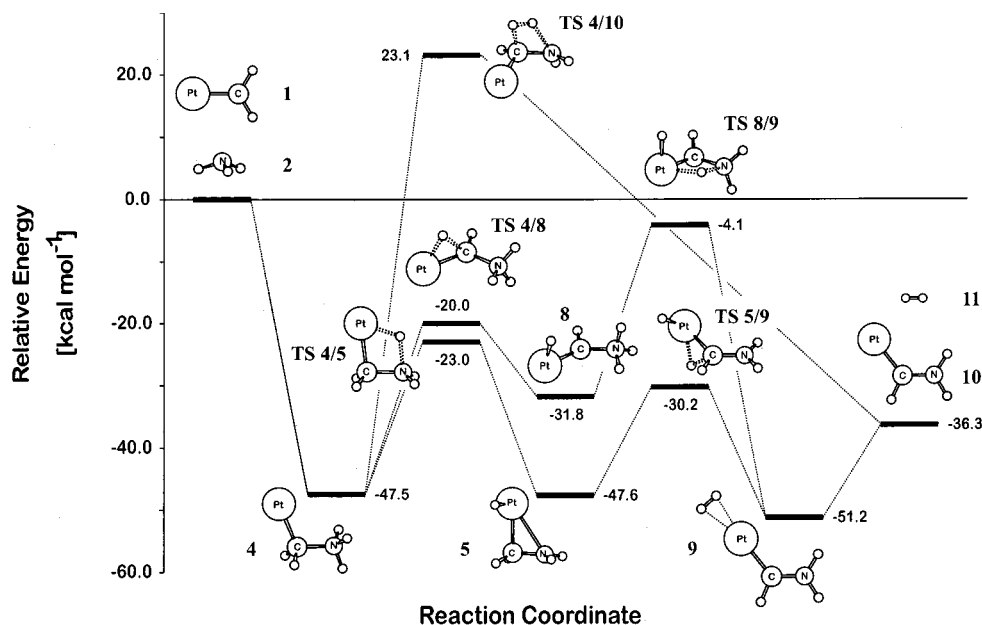
Figure 3. PES of reaction 3b calculated at the B3LYP/TZP//B3LYP/DZP level including ZPVE; charges are omitted.

Figure 1), the carbon−nitrogen bond is already formed. The C−N bond length of 1.54 Å is quite close to that of neutral methylamine (r_{C-N} = 1.47 Å). According to NBO analysis, the Pt−C interaction changes from a double to a single bond on going from **3** to **4**. Along this line of reasoning, the Pt−C bond length increases by about 0.13 Å on going from **3** to **4**. Direct formation of **4** from PtCH$_2^+$ and NH$_3$ can be regarded as the gas-phase analogue of the well-known addition of nucleophiles to Fischer-type carbenes in the condensed phase.[40] The positive charge on **4** is located mostly at the NH$_3$ fragment ($q_N > q_{Pt}$), while the unpaired electron resides on Pt ($\rho_{Pt} > \rho_N$). Accordingly, **4** is best described as an organometallic distonic ion, viz., ·Pt−CH$_2$−$^+$NH$_3$.

En route to the products, next a hydrogen atom is transferred from nitrogen to platinum via the C_s-symmetrical **TS 4/5**. This process is best viewed as a simple proton transfer from nitrogen to platinum, transferring the positive charge to the metal. The most pronounced change in geometry—apart from hydrogen migration—is the decrease of the Pt−C−N angle from 114° toward 97° in **TS 4/5**, so that Pt, C, N, and the migrating hydrogen span a roughly rectangular four-membered ring. Structure **5** is the product minimum for loss of PtH in reaction 3a; this species can be described as a complex between PtH and a formiminium ion, as indicated by the geometrical parameters of the methylene unit. The Pt−C−N angle is only 91°, and the CH$_2$NH$_2$ moiety is almost planar, which points toward an sp^2 hybridization on carbon and a three-center d$_\pi$p$_\pi$ coordination involving Pt, C, and N. While the positive charge shifts from Pt to N and vice versa, it is noteworthy that the unpaired electron in all intermediates of reaction 3a is, by and large, located on Pt ($\rho_{Pt} \approx 0.8$, Table 3). The overall reaction to yield **6** + **7** is exothermic by 23 kcal mol^{-1} relative to the entrance channel. According to NBO analysis, the cationic product **6** has a C−N double bond, and the C−N bond length of 1.28 Å is ca. 0.1 Å shorter than that in **5**. Neutral PtH is formed concomitantly, and its bond energy is calculated to be D_0(Pt−H) = 78 kcal mol^{-1}. This number compares well with that predicted by Wittborn and Wahlgren[41] at the Douglas−
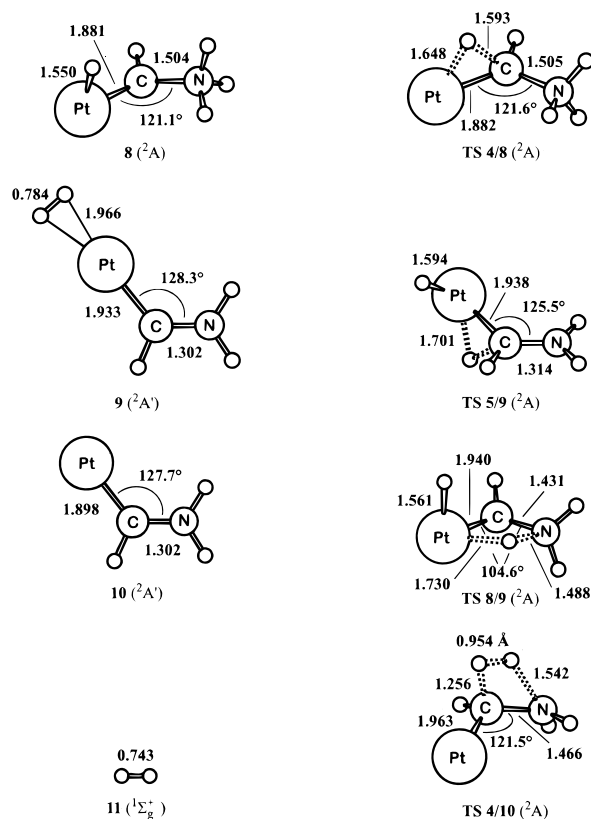

Figure 4. Calculated structures involved in reaction 3b. Bond lengths are given in angstroms and angles in degrees; electronic states are in parentheses.

Kroll/modified coupled pair functional (DK-MCPF) level, i.e., D_0(Pt−H) = 74 kcal mol^{-1}.

In reaction 3b, molecular hydrogen is liberated upon reaction of PtCH$_2^+$ and NH$_3$ to afford the aminocarbene PtC(H)NH$_2^+$ (Figures 3 and 4). In the initial step, we assume formation of **4** either directly or via **3** as described above. Figure 3 shows three possible reaction pathways for H$_2$ elimination commencing from **4**: (i) direct 1,2-elimination from carbon and nitrogen without involving the platinum center, (ii) a 1,2-hydrogen shift from carbon to platinum, followed by a 1,3-shift of hydrogen from

(40) Elschenbroich, C.; Salzer, A. *Organometallics: A Concise Introduction*, 2nd ed.; VCH: Weinheim, 1992.
(41) Wittborn, C.; Wahlgren, U. *Chem. Phys.* **1995**, *201*, 357.

N to Pt, and (iii) a 1,3-shift from N to Pt, followed by a 1,2-shift from C to Pt. While in paths ii and iii platinum is involved directly and exploited as a "catalyst" because all stationary points lie below the entrance channel, **TS 4/10** for the direct 1,2-elimination of hydrogen across the C−N unit is 23 kcal mol^{-1} above the energy of the reactants and therefore considered to be irrelevant. Exclusion of a direct route for the elimination also corroborates the notion that such a process is formally symmetry-forbidden.[42−45] In contrast, according to the calculations, paths ii and iii are below the PtCH$_2^+$ + NH$_3$ entrance channel. The 1,2-hydrogen shift via **TS 4/8** in path ii is associated with an activation barrier of 28 kcal mol^{-1} relative to **4**, and a second hydrogen shift from **8** to the platinum aminocarbene−dihydrogen complex **9** needs to overcome yet another 28 kcal mol^{-1} barrier via **TS 8/9**, which is thus separated from the entrance channel by only −4 kcal mol^{-1} (Figure 3). Complex **9** resides in a deep well (51 kcal mol^{-1} below the reactants) and is separated from the products by 15 kcal mol^{-1} through simple liberation of the H$_2$ unit. Structures **TS 4/5**, **5**, and **TS 5/9** of path iii are geometrically much less strained and lie thus well below the entrance channel, as do the corresponding structures **TS 4/8**, **8**, and **TS 8/9** of path ii. The destabilization of the latter three species is manifested in the high spin density on carbon ($\rho_C \approx 0.7$). Accordingly, path iii is assumed to predominate in the PtCH$_2^+$/NH$_3$ system en route to dehydrogenation. Note that **5**, the intermediate after 1,3-hydrogen shift of path iii, is also the central intermediate in reaction 3a discussed above. Therefore, once **5** is formed from the PtCH$_2^+$/NH$_3$ couple, a competition between simple dissociation by loss of neutral PtH and rearrangement involving a 1,2-hydrogen shift via **TS 5/9** to structure **9** and subsequent loss of H$_2$ is likely to take place. In the final product, **10**, of reaction 3b, the partial charges are nearly equally distributed between Pt and the aminocarbene ligand. The perfect planarity of platinum aminocarbene cation points toward π-bond delocalization in terms of the two resonance structures, $^+$Pt=CH−NH$_2$ ↔ Pt−CH=$^+$NH$_2$.

Structural Aspects. Several [Pt,C,N,H$_3$]$^+$ isomers located as minima are shown in Figure 5. The platinum aminocarbene **10** is the most stable structure, followed by the bisligated complex **14**, which is only 7 kcal mol^{-1} higher in energy. The H−Pt bonded structures **12** and **13** are 19 and 27 kcal mol^{-1} less favorable than **10**, respectively. Another species with Pt−N−C connectivity, **16**, lies 18 kcal mol^{-1} above **10**. The least energetically favorable structures are the η^2-bridged platinum formimine complex **17** and the insertion isomers **18** and **19**, which are 33, 60, and 71 kcal mol^{-1} higher in energy than **10**, respectively. Accordingly, the experimentally deduced carbene structure also appears to be the thermochemically most stable one. Note, however, that the observed specifity of the labeling experiments rules out participation of **14**, **16**, **17**, and **19** in reversible steps.

It is also instructive to compare the platinum carbene PtCH$_2^+$ **1** with its mono- and diamino derivatives PtC(H)NH$_2^+$ **10** and PtC(NH$_2$)$_2^+$ **20** (Figure 6). At the first, counterintuitive view, the Pt−C bond lengths elongate upon amino substitution ($r_{Pt−C}$ = 1.83, 1.90, and 1.94 Å in **1**, **10**, and **20**, respectively). This geometric effect can be attributed to Coulomb repulsion in that the donor properties of the amino ligands enhance build-up of
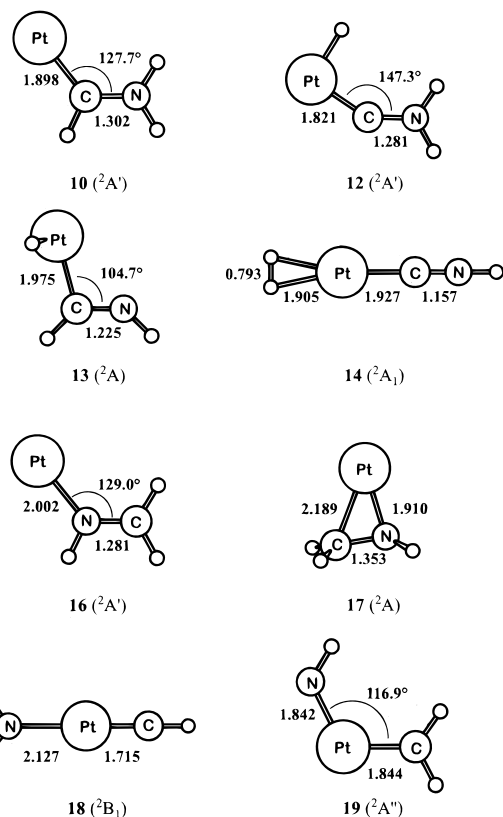

Figure 5. Calculated minima of isomers of the [Pt,C,N,H$_3$]$^+$ cation. Bond lengths are given in angstroms and angles in degrees; electronic states are in parentheses.
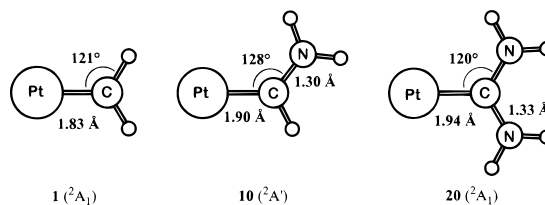

Figure 6. Calculated minima of platinum carbene PtCH$_2^+$ and its amino derivatives PtC(H)NH$_2^+$ and PtC(NH$_2$)$_2^+$. Bond lengths are given in angstroms and angles in degrees; electronic states are in parentheses.]

positive charge on the carbon centers, thereby affecting the Pt−C bond. This argument is nicely corroborated by NBO analysis, which predicts q_{Pt} = 0.71 in **1**, 0.53 in **10**, and 0.47 in **20**. The platinum−carbene bond strengths, however, increase by about 12 kcal mol^{-1}, i.e., D_0(Pt$^+$−CH$_2$) = 118 kcal mol^{-1} vs D_0(Pt$^+$−C(H)NH$_2$) = 130 kcal mol^{-1} and D_0(Pt$^+$−C(NH$_2$)$_2$) = 129 kcal mol^{-1}, which resembles nicely the stabilization of the carbene ligand with increasing heteroatom substitution.[46,47] In the platinum diaminocarbene **20**, the effect of Pt−C bond stabilization is counteraffected by the stabilization in the separated diaminocarbene. The more pronounced effect in the Pt−C bond energy for the monosubstituted platinum aminocarbene is also manifested in the isodesmic reaction 2PtC(H)NH$_2^+$ → PtCH$_2^+$ + PtC(NH$_2$)$_2^+$, which is 26 kcal mol^{-1} endothermic, thus favoring the monoaminocarbene **10**.

PES of Dehydrogenation of PtC(H)NH$_2^+$. Loss of molecular hydrogen from **10** may occur on two different reaction paths, which both involve consecutive hydrogen shifts (Figures

(42) Williams, D. H.; Hvistendahl, G. *J. Am. Chem. Soc.* **1974**, *96*, 6753.

(43) Vulpius, T.; Øiestad, E. L.; Øiestad, Å. M. L.; Skaane, H.; Ruud, K.; Helgaker, T.; Uggerud, E. *Eur. Mass Spectrom.* **1995**, *1*, 121.

(44) Uggerud, E.; Øiestad, Å. M. L. *Int. J. Mass Spectrom. Ion Processes* **1997**, *167/168*, 117.

(45) Fleming, I. *Grenzorbitale und Reaktionen organischer Verbindungen*, 2nd ed.; VCH: Weinheim, 1990.

(46) Herrmann, W. A.; Köcher, C. *Angew. Chem.* **1997**, *109*, 2257.

(47) Heinemann, C.; Müller, T.; Apeloig, Y.; Schwarz, H. *J. Am. Chem. Soc.* **1996**, *118*, 2023.
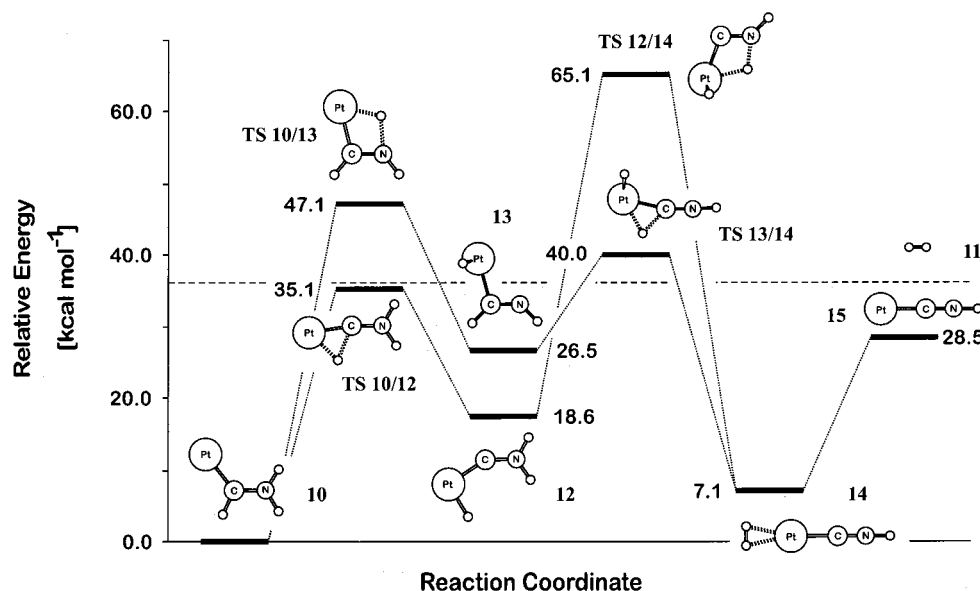
Figure 7. PES of H$_2$ loss from platinum aminocarbene PtC(H)NH$_2^+$ (**10**) calculated at the B3LYP/TZP//B3LYP/DZP level including ZPVE. The dashed horizontal line at 36.3 kcal mol^{-1} represents the relative energy of the PtCH$_2^+$ + NH$_3$ entrance channel as a reference; charges are omitted.
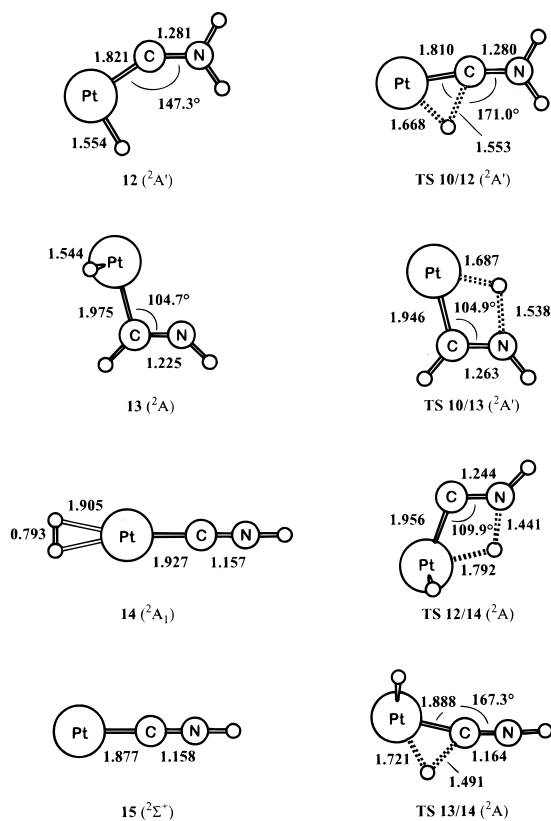

Figure 8. Calculated structures of the species involved in Figure 7. Bond lengths are given in angstroms and angles in degrees; electronic states are in parentheses.

7 and 8). Overall, the dehydrogenation **10** → **15** is endothermic by 29 kcal mol^{-1} and associated with considerable barriers. Again, the energetically less demanding path consists of a 1,3-hydrogen shift, followed by a 1,2-hydrogen shift, i.e., **10** → **13** → **14**. For the alternative route, i.e., **10** → **12** → **14**, the highest barrier (**TS 12/14**) amounts to 65 kcal mol^{-1} relative to **10**; this is 29 kcal mol^{-1} above the PtCH$_2^+$/NH$_3$ entrance channel. Nevertheless, also for the more favorable path, the highest barrier, **TS 10/13**, is 11 kcal mol^{-1} higher in energy than the separated reactants PtCH$_2^+$ and NH$_3$. Thus, even though the

overall reaction PtCH$_2^+$ + NH$_3$ → PtCNH$^+$ + 2H$_2$ is exothermic by 8 kcal mol^{-1}, it is hindered by the barrier associated with the 1,3-hydrogen shift via **TS 10/13**. This theoretical result is entirely consistent with the experimental findings described above, i.e., PtCH$_2^+$ + NH$_3$ does not spontaneously afford formation of [Pt,C,N,H]$^+$, while this particular channel is accessed for the isomeric Pt$^+$/CH$_3$NH$_2$ couple, which is calculated to be 35 kcal mol^{-1} higher in energy. This number is somewhat larger than the experimental difference in entrance energies of 25 kcal mol^{-1}.[29-31] However, spin−orbit splitting is substantial in Pt$^+$; given that the separation of the $^2D_{5/2}$ and $^2D_{3/2}$ levels amounts to 24 kcal mol^{-1},[48] the weighted average applied in our RECP approach lies 9 kcal mol^{-1} above the $^2D_{5/2}$ ground level. In addition, the weighted average of PtCH$_2^+$ lies 4 kcal mol^{-1} above the $^2A_1$ ground level.[31] Thus, upon inclusion of this first-order spin−orbit effect, the difference in entrance energies reduces to 30 kcal mol^{-1}, which is in acceptable agreement with the experimental number.

Interestingly, the Pt−N-bonded platinum HCN complex PtNCH$^+$ (r_{Pt-N} = 1.93 Å, r_{N-C} = 1.15 Å) is predicted to be 13 kcal mol^{-1} less stable than the platinum isonitrile complex PtCNH$^+$, although the heat of formation of HNC is 16 kcal mol^{-1} higher than that of HCN[29] (14 kcal mol^{-1} at B3LYP level). Platinum cation is bound more strongly to the ligand in the Pt−isonitrile isomer by 26 kcal mol^{-1}, i.e., D_0(Pt$^+$−CNH) = 89 kcal mol^{-1} vs D_0(Pt$^+$−NCH) = 63 kcal mol^{-1}. Platinum cation acts thus as a stabilizing ligand for the isonitrile isomer. Additionally, CID of [Pt,C,N,H] shows that regeneration of Pt$^+$ and liberation of HCN/HNC is feasible. Although unimolecular HNC/HCN isomerization is hampered by large barriers,[49,50] acid/base-catalyzed isomerizations are easily conceivable.[51]

5. Discussion

Reactions 3a and 3b. Formation of CH$_2$NH$_2^+$ constitutes the major product channel in the reaction of PtCH$_2^+$ and NH$_3$.

(48) Moore, C. E. *Atomic Energy Levels*; National Standard Reference Data Series NSRDS-NBS 35; National Bureau of Standards: Washington, DC, 1971.

(49) Koch, W.; Frenking, G.; Schwarz, H. *Naturwissenschaften* **1984**, *71*, 473.

(50) Palma, A.; Semprini, E.; Stefani, F.; Talamo, A. *J. Chem. Phys.* **1996**, *105*, 5091.

(51) Bouchoux, G.; Nguyen, M. T.; Longevialle, P. *J. Am. Chem. Soc.* **1992**, *114*, 10000.

Our calculations predict reaction 3a to be exothermic by 23 kcal mol^{-1}, which is in line with the fact that, under FTICR conditions, only exothermic reactions should occur for thermalized ions. Furthermore, theory and experiment are in concert in that both **TS 3/4** and **TS 4/5** are predicted to be well below the entrance channel. Calculations on the PES of reaction 3b also agree nicely with the experimental results, in that all intermediates of paths ii and iii are below the energy of the entrance channel. As mentioned in section 4, path i is energetically unfavorable. It does not contribute to loss of H$_2$ due to the fact that **TS 4/10** is well above the energy of the entrance channel and hence is not accessible within the experimental energy frame. Interestingly, loss of H$_2$ to yield PtC(H)NH$_2^+$ is less efficient than reaction 3a, although the calculations predict channel 3b to be 13 kcal mol^{-1} more exothermic, and the associated barriers are lower than or close to the energy requirements of reaction 3a. Thus, branching in favor of reaction 3a cannot be solely attributed to energetic criteria, as the intermediates in reaction 3a and in the least energy demanding path iii of reaction 3b are identical until the formation of **5**. However, while reaction 3a can proceed directly in a simple dissociation to produce PtH and CH$_2$NH$_2^+$, in the dehydrogenation of **5** another entropically demanding step, i.e., the 1,2-hydrogen shift via **TS 5/9**, has to occur en route to H$_2$ loss, passing through structure **9**. As the density of states and thus the lifetime of **TS 5/9** is likely to be relatively small, passing such a "tight" transition structure can be assumed to be less efficient compared to direct, energetically viable dissociation of **5** into CH$_2$NH$_2^+$, along with neutral PtH. Therefore, the experimental product branching ratio primarily reflects the kinetic restrictions associated with reactions 3a and 3b rather than the relative thermochemistry.

Moreover, thermal contributions need to be considered. Dissociation of **5** into PtH + CH$_2$NH$_2^+$ affords two particles, compared to the unimolecular rearrangement via **TS 5/9**. To estimate the effect of finite temperature by considering the calculated PESs at 298 K, based on the energy of the entrance channel, the effective temperature of intermediate **5** is much larger. Inclusion of thermal effects does not alter the relative energetics of the PESs significantly (<2 kcal mol^{-1}), except for the exit channels, which experience a drastic stabilization due to entropy contribution. In fact, at 298 K, the Gibbs free energy of the exit channel (−22 kcal mol^{-1} relative to PtCH$_2^+$ + NH$_3$) is even below that of **TS 5/9** at this temperature (−21 kcal mol^{-1}). Accordingly, the observed preference of reaction 3a is quite obvious under the experimental conditions in the gas-phase experiments.

Formation of PtCNH⁺. Dehydrogenation of PtC(H)NH$_2^+$ leads to a PtCNH$^+$ cation, which may eventually yield HCN upon dissociation as the desired product in the Degussa process. However, although the net dehydrogenation of PtC(H)NH$_2^+$ is exothermic ($\Delta_r H = -8$ kcal mol^{-1} for the reaction PtCH$_2^+$ + NH$_3 \rightarrow$ PtCNH$^+$ + 2H$_2$), both of the two alternative pathways in this reaction are hindered by considerable barriers (Figure 7). Thus, if the energetically less demanding path via **10** → **TS 10/13** is chosen, the transition state must lie at least 11 kcal mol^{-1} above the entrance channel given by **1** and **2**. This computational view of the PES is in agreement with the fact that PtCNH$^+$ is not formed from the PtCH$_2^+$/NH$_3$ couple under thermal conditions, whereas PtCNH$^+$ is observed upon raising the entrance energy by means of exchanging the PtCH$_2^+$/NH$_3$ couple with Pt$^+$/CH$_3$NH$_2$.

Implication for the Degussa Process. The Pt$^+$/CH$_4$/NH$_3$ system can serve as a functional model for the Pt-catalyzed

coupling of methane and ammonia in the Degussa process. The gas-phase model shows a favorable selectivity in that bare Pt$^+$ reacts much faster with methane than ammonia, whereas the opposite holds true for PtCH$_2^+$. According to the calculations, the reaction profile evolves from the encounter complexes **3** and **4** to the C−N coupling product **5** via attack of ammonia at the carbene moiety. Structure **5** serves as a central intermediate from which the major product channels evolve.

Reaction 3a gives rise to the liberation of an iminium ion, CH$_2$NH$_2^+$, into the gas phase, which can subsequently be deprotonated to afford neutral formimine. The latter is an immediate precursor for HCN. Conceptually, proton abstraction from the iminium ion concomitant with formation of PtH as a formal metal hydride can be regarded as a stepwise dehydrogenation, eventually yielding molecular hydrogen, i.e., H$^+$ + H$^- \rightarrow$ H$_2$. Similar protonation/deprotonation and hydride-transfer sequences can also provide a low-energy path for the dehydrogenation of formimine to cyanic acid. Such bi- or termolecular, stepwise variants would circumvent the appreciable barrier of 93 kcal mol^{-1} associated with the corresponding unimolecular processes of formal 1,2-hydrogen eliminations.[52] From a thermochemical point of view, dehydrogenation of formimine imposes no major constraint en route to cyanic acid, because the reaction CH$_2$NH → HCN + H$_2$ is more or less thermoneutral.

In contrast, platinum is actively involved in the dehydrogenation sequence commencing with reaction 3b. A key step is the formation of the aminocarbene **10** via a nucleophilic attack at the carbon, followed by substitution of NH$_2$ for H. In nice agreement of the experimental and theoretical results, the barriers associated with the subsequent dehydrogenation **10** → PtCNH$^+$ + H$_2$ are too high to be surmounted in the Pt$^+$/CH$_4$/NH$_3$ system at thermal energies, but they can be passed at elevated energies, e.g., upon CID or starting from the Pt$^+$/CH$_3$NH$_2$ couple. Thus, the energy demand of the overall cyanic acid synthesis is, by and large, concentrated upon the final dehydrogenation step and product desorption in particular. Moreover, product desorption must involve isomerization of the more stable isonitrile complex into cyanic acid, which is the more stable isomer in the gas phase. Again, this process is unlikely to occur unimolecularly but is expected to be quite facile in a protonation/deprotonation sequence.[51]

Accordingly, one major implication of the model system is that generation of HCN can proceed via two different routes. Both commence with the Pt-mediated activation of methane, followed by attack of the ammonia at the methylene group, but then bifurcate into two competing routes for the generation of HCN. Thus, reaction 3a leads to the liberation of formimine, which may then undergo dehydrogenation in the gas phase without further metal catalysis, whereas reaction 3b initiates a surface-bound pathway via aminocarbenes. Figure 9 gives a simplified sketch of the proposed elementary steps.

The mechanistic scenario with two competing routes for HCN genesis implies at least bimodal temperature and pressure profiles of the Degussa process due to the different thermodynamic characteristics of the gas-phase route and the surface-bound process. The validity of this mechanistic scenario in the Degussa process might be probed by comparison with the degradation of methylamine on Pt contacts[53,54] because the branching ratios between reactions 3a and 3b differ in the Pt$^+$/

(52) For possible variants of such stepwise dehydrogenations, see footnote 12 in ref 6.
(53) Hwang, S. Y.; Schmidt, L. D. *J. Catal.* **1988**, *114*, 230.
(54) Hwang, S. Y.; Kong, A. C. F.; Schmidt, L. D. *J. Phys. Chem.* **1989**, *93*, 8327.
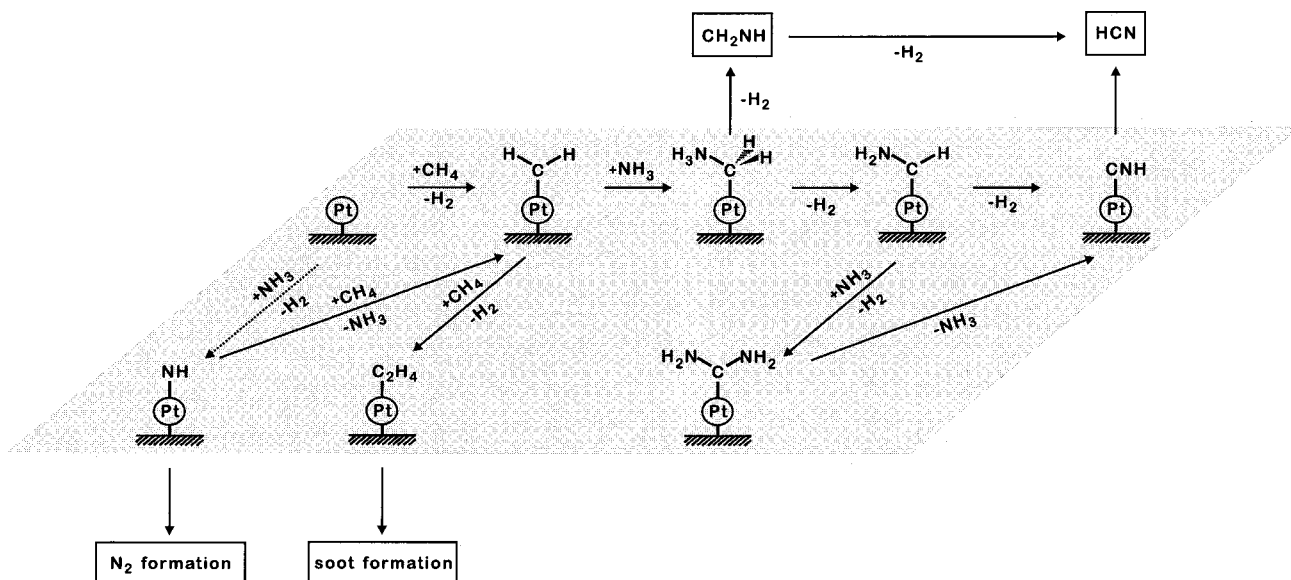
Figure 9. Schematic representation of elementary steps involved our model system for the Degussa process (see text).

CH_4/NH_3 and Pt^+/CH_3NH_2 systems. If the proposed set of elementary steps also holds true in the Degussa process, notable effects are to be expected upon changing the substrate from CH_4/NH_3 to CH_3NH_2.

Further implications can be derived from consideration of the other reactions observed experimentally. Thus, as already mentioned above, activation of ammonia by Pt^+ is much more difficult than that of methane. Moreover, even if Pt−imine species were formed on the catalyst, the high efficiency of reaction 6 suggests their rapid return into the catalytic sequence in the presence of methane. Moreover, considering that Pt−imines are likely precursors for the thermal decomposition of ammonia to nitrogen, the removal of the imine ligands by metathesis with methane suggests that the rate of Pt-catalyzed ammonia decomposition decreases upon addition of methane. Increasing the partial pressure of methane, of course, also enhances the risk of soot formation and thus passivation of the catalyst. In the gas-phase mode, this step is represented by the formation of $Pt(C_2H_4)^+$ according to reaction 4, which, however, cannot compete with C−N bond coupling in reaction 3 unless methane and ammonia are present in a 1:1 ratio. The CID experiments performed with **20** suggest that diaminocarbenes are no sink in the catalytic cycle under the conditions of the Degussa process, because collisional activation of **20** inter alia affords HCN.

Finally, let us comment on the particular role of platinum for CH_4/NH_3 bond coupling compared to the other metals investigated here. Except for $FeCH_2^+$ and $CoCH_2^+$, all metal carbenes examined in this study can bring about C−N bond coupling with NH_3. Thus, attack of the methylene group by ammonia is not unique to platinum. Similarly, also 5d metal cations other than Pt^+ can bring about activation of methane at thermal energies, namely, W^+, Os^+, Ir^+, and Pt^+;[23,24] note, however, that the reactivity of ground-state W^+ toward CH_4 has been questioned.[55] In the combination of methane and ammonia activation, however, the Pt^+ system is most efficient among these elements. Thus, Fe^+, Co^+, Rh^+, and Au^+ are incapable of activating either methane or ammonia and thus fail in the initiating step.[34] Dehydrogenation of methane by M^+ to afford MCH_2^+ occurs with comparable rates for W^+, Ir^+,

Os^+, and Pt^+. For WCH_2^+ and $IrCH_2^+$, however, successive reactions to induce methane oligomerization are facile.[23,24] These C−C bond couplings may be regarded as an indication for catalyst passivation via soot formation, and similar arguments can be raised for the pronounced neutral MCH products with M = Os and Ir. Further note that the high oxophilicity of tungsten very much limits the perspectives of low-valent tungsten catalysts. Thus, platinum combines two properties in a favorable manner: (i) the ability to activate methane but not ammonia and (ii) preferential attack of the metal carbene by ammonia rather than methane.

6. Conclusions

In the present study, the $Pt^+/CH_4/NH_3$ system is probed in detail by experiment and theory. In general, the agreement between the theoretically predicted PES and the experimental results for C−N bond formation is good, if not fortuitously excellent. This lends confidence to the reliability of the chosen B3LYP/RECP/TZP//RECP/DZP approach for semiquantitative computational studies of reaction mechanisms in medium-sized organometallic systems involving platinum as a heavy metal atom.

For the gas-phase modeling of the Degussa process, the extension of the present system to neutral[56] and anionic Pt atoms as well as to small Pt clusters[57,58] is desirable. Considering the "real" heterogeneous process, the gas-phase experiments suggest that it might be interesting to investigate the role of positive partial charges on the catalyst.

However, these implications, derived from the present gas-phase study, apply only to the outlined scenario of elementary steps for mononuclear transition metals. In practice, however, metal clusters may play major roles and may change reactivity patterns fundamentally.[59] For example, while bare Rh^+ as well as rhodium clusters Rh_n^+ (n = 3−10) do not activate methane, Rh_2^+ affords $Rh_2CH_2^+$ with a remarkable efficiency (ϕ = 0.7).[60] Interestingly, however, coupling of methane and ammonia is

(55) Kikhtenko, A. V.; Goncharov, V. B.; Momot, K. I.; Zamaraev, K. I. *Organometallics* **1994**, *13*, 2536.

(56) Carroll, J. J.; Weisshaar, J. C.; Siegbahn, P. E. M.; Wittborn, C. A. M.; Blomberg, M. R. A. *J. Phys. Chem.* **1995**, *99*, 14388.
(57) Jackson, G. S.; White, F. M.; Hammill, C. L.; Clark, R. J.; Marshall, A. G. *J. Am. Chem. Soc.* **1997**, *119*, 7567.
(58) Niedner-Schatteburg, G.; Bondybey, V. E.: Unpublished results.
(59) Heiz, U.; Sanchez, A.; Abbet, S.; Schneider, W.-D. *J. Am. Chem. Soc.* **1999**, *121*, 3214.

less efficient for Rh/Pt compared to pure platinum.[61] Our results must, therefore, be understood as a mechanistic guidance rather than in terms of providing accurate descriptions of how the active catalysts works in the applied processes.

(60) Albert, G.; Berg, C.; Beyer, M.; Achatz, U.; Joos, S.; Niedner-Schatteburg, G.; Bondybey, V. E. *Chem. Phys. Lett.* **1997**, *268*, 235.

(61) Bockholt, A.; Harding, I. S.; Nix, R. M. *J. Chem. Soc., Faraday Trans.* **1997**, *93*, 3869.

(62) Su, T.; Chesnavich, W. J. *J. Chem. Phys.* **1982**, *76*, 5183.

(63) Su, T. *J. Chem. Phys.* **1988**, *88*, 4102.

(64) Su, T. *J. Chem. Phys.* **1988**, *89*, 5355.

(65) Huber, H. P.; Herzberg, G. *Constants of Diatomic Molecules*; Van Nostrand-Reinhold: New York, 1979.

JA992642W